ELECTRIC SLAG FURNACE DIMENSIONING

Mark William Kennedy

Norwegian University of Science and Technology, Department of Materials Science and Engineering, N-7491 Trondheim, Norway

mark.kennedy@material.ntnu.no

Keywords: Slag, resistance, furnace, dimensioning, scale-up

Abstract

Electric furnaces containing high quantities of slag are applied in many areas of pyrometallurgy, often for smelting or slag cleaning. A variety of ratios or rules of thumb have been employed in the industry for the dimensioning of these vessels, in most cases with no clear technical basis.

In this paper, several design guidelines are presented (electrode size, spacing, vessel dimensions, energy intensity, etc.) as an attempt to provide some technical basis for optimal dimensioning.

Furnace heat generation is related to side wall copper cooler heat losses, in an attempt to establish a methodical design strategy particularly for minimum electrode to wall spacing for modern furnaces with cooled linings.

Issues regarding the true nature of heat production in a slag furnace are discussed with regards to the possible impact on accurate modeling and design.

Introduction

Slag furnaces have passed through a number of design 'generations' characterized by increasing energy intensities, improved electrode technologies and advancing development in their physical structure or 'furnace integrity' as shown in Table I [1]. A 3rd generation furnace using ultra-high-power (UHP) graphite electrodes is shown in Figure 1, as a generic example of the types of physical structures present in modern slag furnace designs [1].

Table I. Slag Furnace Generations, Energy Intensities and Physical Characteristics [1]

Furnace Generation	Energy Intensity (kW/m^2 of hearth area)	Typical Characteristics
1	~100	Immersed electrodes, shell film cooling
2	~200	Brush arc and plate or bath-line coolers
3	300-400	Shielded arc with finger, plate or bath-line coolers
4 (under development)	500-1000	Fully cooled slag zone, additional cooled structures to maintain vessel integrity (e.g. metal zone, tapholes, etc.).

Generation 1 furnaces have a very low energy intensity (<100 kW/m^2), a large bath area and, therefore, a correspondingly large outer surface area for a given power input. For any given surface heat flux, this large outer area leads to higher furnace heat losses and relatively low thermal efficiencies. This has driven furnace designers to build higher powered furnaces with greater energy intensity or to increase the power input to existing furnaces. Both have the effect of minimizing the heat losses as a percentage of the total power input and thereby achieving improved thermal efficiencies. As a first approximation, the slag zone heat losses as a fraction of the total furnace power should vary inversely with the furnace diameter (D_f), i.e. proportional to D_f/D_f^2 or D_f^{-1} for a fixed slag depth and bath power intensity.

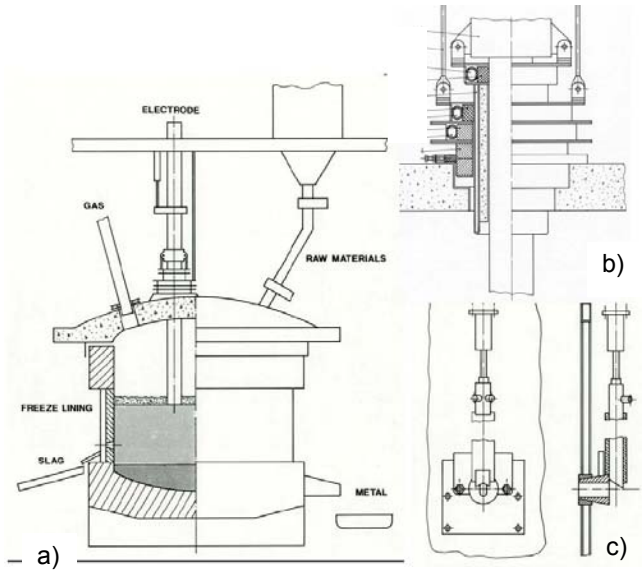

Figure 1. Overview of some furnace details. a) Elkem Multi-Purpose Furnace®, b) electrode seal, and c) slag flow controller [2].

As furnace slag bath energy intensity has increased, slag superheat has risen, distance to the side lining has fallen, and hence refractory erosion in the slag zone has accelerated. At sidewall heat fluxes >15-20 kW/m^2, high conductivity refractory and shell water film cooling no longer provides adequate cooling, due to the formation of dry spots. 2nd and 3rd generation furnaces, therefore, include bath-line coolers to ensure a slag freeze lining and maintain the furnace integrity, as indicated in Table I. A modern bath-line cooler is shown in Figure 2 [3].

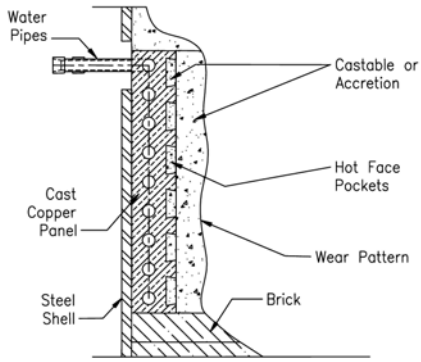

Figure 2. Water cooled slag furnace copper cooler with a hot face pattern [3].

Slag Furnace Basic Design

In the basic design of a slag furnace a series of steps are typically followed:

1. A target furnace production rate (PR) is chosen [kg/h],
2. Specific energy requirement (SER) of the process is established based on thermodynamic analysis or known benchmark data (excluding heat losses) [Wh/kg],
3. The smallest reasonable electrode diameter is selected [m], along with the number and type,
4. Initial furnace dimensions are chosen based on an acceptable energy intensity as indicated in Table I [W/m^2] or by standard ratios to the electrode dimensions,
5. Furnace heat losses are estimated [W], and
6. The total furnace power verified [W] or in more practical units [MW].

These design steps often require iteration to arrive at a 'converged' basic concept. The selection of electrode size and application of standard ratios may result in too high or low a furnace energy intensity. Current density may be too high for the selected electrodes and this may force the selection of larger diameter or better quality electrodes, greater number, and an alternate furnace shape or dimensions to accommodate them.

Steps 1. and 2. will not be discussed in detail as they are project specific; however, the furnace production rate should include factors for down time, reduced throughput operation and the required catch up rate. The SER should treat the off-gas from the furnace as a process stream, it is not a loss, anymore than the slag stream is a loss. The impact of air infiltration and/or off-gas combustion in the furnace freeboard on the overall heat balance is complex, but should be evaluated if possible. When evaluating the thermodynamic specific energy requirement, care must be given to estimating the total heat capacity of the slag and matte phases accounting for sensible heat, phase changes and heats of mixing in the liquid phase. These can be modeled conveniently using commercial thermodynamic software packages. It is important to benchmark the modeling results against industrial data [4] or direct measurements. Software alone is insufficient to ensure an accurate design.

Furnace Configuration and Electrode Selection

The electrical design (e.g. resistance estimation) of slag furnaces is addressed in a related paper [5]; however, electrode sizes relate directly to furnace dimensioning through the use of scaling ratios and must, therefore be addressed in some detail. Søderberg, carbon and graphite electrodes will be discussed.

Different types of electrodes have different current carrying capacities, as determined by their physical and chemical properties and established by empirical experience (due to burning, breakage, consumption rate, etc.). For a fixed furnace resistance, the limiting current sets an upper MW/electrode and this establishes the required number of electrodes for a given furnace power. Once an electrode size and number are selected, the furnace is effectively dimensioned if standard ratios are applied to the electrode diameter (D_e). The resulting electrode number (typically 1, 2, 3 or 6 as indicated in Figure 3) or furnace size may not be as desired by the designer, who may then select a new electrode size. Given that the electrode to furnace bottom resistance is ~inversely proportional to the electrode diameter, i.e. D_e^{-1} [5], the design task then becomes iterative.

Typical slag furnace body and electrode configurations are pictured in Figure 3. A typical electrode spacing (S_e), measured centre-to-centre of $2.7D_e$ [6] along with an electrode to wall spacing of $1.6D_e$ is used in Figures 3 a) through c) [7]. A total furnace diameter of $7.7D_e$ is used in Figure 3 c) and the circle pitch diameter (CPD) of the electrodes is shown, where CPD = $2S_e/\sqrt{3}$. In Figure 3 d) a 6-in-line furnace is shown, with width $6D_e$ and length $21D_e$ [6].

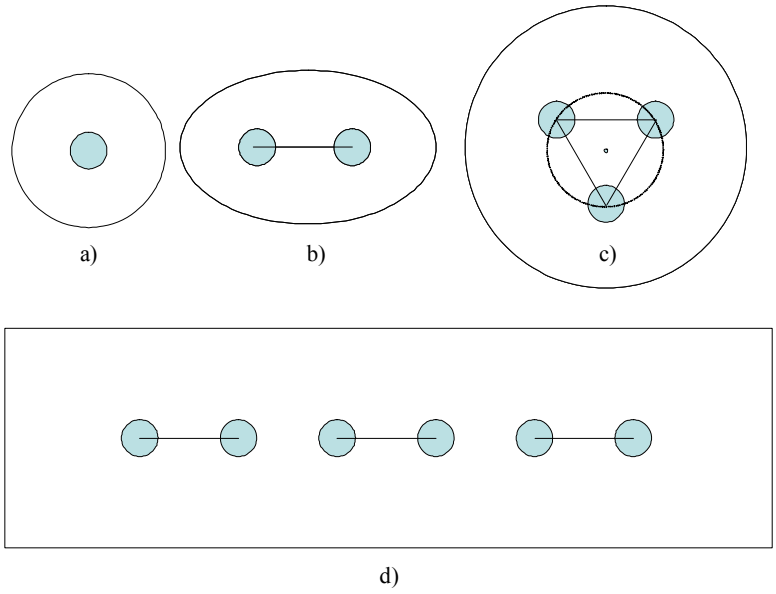

Figure 3. Typical electric furnace electrode and furnace body arrangements:
a) single top entering electrode (1-phase), b) two electrodes (1-phase), c) three electrodes (3-phase) and d) six-in-line electrodes (3-single phase).

Carbon Electrodes (Søderberg and Pre-baked)

Self baking Søderberg electrodes [8] have traditionally been used in many slag furnace designs since the 1920's. Søderberg electrodes have current density limitations typically in the range of 4 – 7 A/cm^2 [9], with an indicative electrical resistivity of 3.33 x10^{-5} Ωm at 1500^{o}C [10]. They have low operating cost and are highly suitable for furnaces with low energy intensity, such as 1st or 2nd generation designs (i.e. ~100-200 kW/m^2), as the low electrode current density results in a large electrode diameter, for a given power input. Data for pre-baked carbon electrodes are sparse, but they have similar electrical resistivity (~3 x10^{-5} Ωm) [11] and current limits (~6 A/cm^2) [12] to Søderberg electrodes.

Current carrying capacity of Søderberg electrodes has been published previously by Westly [9]. The formula is as follows:

$$I_e = C_e \left(\frac{R_{ac}}{R_{dc}} \right)^{-0.5} D_e^{1.5} \qquad (1)$$

where I_e is the total current [kA], C_e is an electrode load factor between 50 and 65 (giving a furnace down time between 0.2 and 2%), R_{ac} is the alternating current resistance of the electrodes [Ω], R_{dc} is the direct current resistance of the electrodes [Ω] and D_e is the diameter of the electrodes [m].

For electrodes up to 1 m in diameter R_{ac}/R_{dc} can be found using the following equations [13]:

$$\frac{R_{ac}}{R_{dc}} = \frac{\xi_e}{2}\left(\frac{ber\xi_e bei'\xi_e - bei\xi_e ber'\xi_e}{ber'^2(\xi_e)+bei'^2(\xi_e)}\right) \tag{2}$$

$$\xi_e = \frac{D_e}{\delta_e\sqrt{2}} \tag{3}$$

$$\delta_e = \left(\frac{\rho_e}{\pi\mu_o\mu_r f}\right)^{0.5} \tag{4}$$

where ξ_e is a dimensionless electromagnetic penetration or reference depth. *Ber*, *ber'*, *bei* and *bei'* are the real and imaginary parts of the zero order modified Kelvin Bessel functions and their derivatives, the solutions to which can be found using numerical solvers or look-up tables [14]. δ_e is the electromagnetic penetration depth [m], ρ_e is the electrical resistivity of the electrode [Ωm], μ_o is the magnetic permeability of the free space (4π x10^{-7} [H/m]), μ_r the relative magnetic permeability [assumed = 1], and f is the frequency [Hz].

For electrodes over 1 m in diameter it has been reported that the proximity effect also becomes important [9]. FEM models showing both effects, have been published for Søderberg electrodes in round 3-phase furnaces [15]. Effects of electrode length, the steel casing and the distribution of the current flow into the slag, have not been included in most FEM or analytical models describing electrode resistance and such models are indicative only.

The effect of skin depth on electrode resistance ratio (R_{ac}/R_{dc}) is plotted in Figure 4, for a number of electrical conductivities spanning the range from Søderberg or pre-baked carbon, through to high quality ultra-high-power (UHP) graphite electrodes. Arbitrarily selecting a limiting ratio of 1.5 corresponds to Søderberg electrodes of ~2.1 m and graphite electrodes of ~0.75 m. Practical upper limits of ~2.0 m and 0.7 m [16-17] are known from industrial practice. If DC current is supplied to the furnace, then Equations (2) to (4) do not apply and larger diameter electrodes can be effectively used.

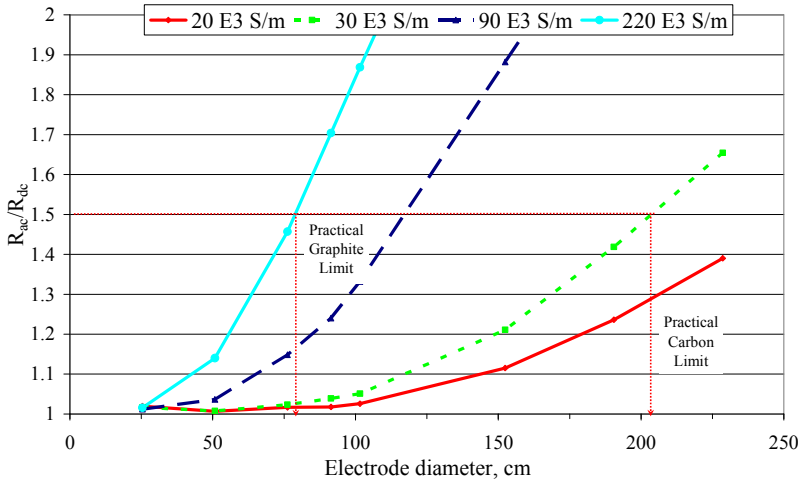

Figure 4. Ratio of R_{ac}/R_{dc} for electrodes at 50 Hz.

Graphite Electrodes

The relative electrical conductivity of graphite varies in a very narrow band from 1 at room temperature, through a range from 0.8 to 1.1, at temperatures between 400 and 1500°C, and, therefore, does not play a major role in establishing the limiting current [16]. According to Equation (1) the allowable electrode current scales by $D_e^{1.5}$, and the allowable current density by $D_e^{-0.50}$. Data from different graphite producers appears to indicate this relation also holds true for high quality graphite electrodes [16-17].

Using the commercially available data for high power graphite electrodes [16-17], size functions can be derived from any single point, such as:

$$J_e = 22D_e^{-0.5} \tag{5}$$

$$I_e = 170D_e^{1.5} \tag{6}$$

where J_e is the electrode current density [A/cm^2].

Electrode Spacing

It has been generally assumed that some ideal electrode spacing exists and is related to the electrode diameter. This idea may have come from the assumption that each electrode has an 'active zone' [18] and that these active zones should not over-lap, i.e. each electrode should operate in an 'independent' crater, in the context of a submerged arc furnace (SAF). Westly recommended that the spacing of the electrodes, like all other furnace dimensions, should vary by the cube root of the furnace power in SAF's [9]. This provides one criterion for 'dimensional similarity' in scale-up. Recent work on ferro-alloy and silicon SAF's has shown that the traditional range of ratios ($S_e \sim 2.4\text{-}3.0D_e$, with 2.7 being accepted as 'typical') is probably not valid and implying that much larger ratios may be advisable [19-21].

In the context of an SAF, too small an electrode spacing will lead to a joining of the craters, structural weakening and collapse, preventing proper preheating and pre-reduction of the charge. It could also lead to too thin a charge layer over the crater and poor recovery of energy and vapors from the off-gas and low overall process thermal efficiencies. Translating these issues into the context of a slag furnace, 'too close' an electrode spacing could be defined as the point where the furnace must operate with an open bath between the electrodes; however, the consequences to slag furnace operation are somewhat different than for an SAF, due to the generally lower reduction duty and associated off-gas volume. The benefits of a smaller furnace diameter and reduced sidewall heat losses, may off-set any increased thermal losses to the freeboard and hotter off-gas, caused by partially open bath operation. Narrow spacing will result in hotter slag near the electrodes, lower resistance, and higher current, lower power factor, may require larger electrodes, hoists, bus bars, and transformers, leading to greater capital cost and potentially lower electrical efficiency.

Experimental investigations using salt models to simulate slag baths have been conducted measuring the voltage and power gradient radiating from an 'immersed' electrode. These results indicated that with simple ionic conduction, the majority of the power is dissipated in a volume defined by about 2 electrode diameters [22]. These results are supported by the work of Jiao, who showed that resistance (or more specifically the geometric constant) in salt models does not vary significantly with electrode spacing greater than $2D_e$, and that deep

electrode immersion further reduces the dependency [23]. An 'active' zone corresponding to a radius of D_e would also imply a minimum electrode to wall spacing of $0.5D_e$ measured from the side of the electrode to the wall (certainly a difficult or impossible to attain minimum).

It is not clear if the 'ideal' electrode spacing concept has ever been validated by any systematic studies in operating slag furnaces. Limited furnace data is available, but it appears to indicate that a much higher impedance region exists in the zone closest to the electrode, than would be predicted assuming simple ionic current flow [24-25]. Whether this is due to gas bubbles, polarization or other interfacial phenomena is not clear. The available data imply that a higher percentage of the power is developed close to the electrode and this would imply a relatively small active region. Until systematic measurements of complex impedance are made using neutral measuring electrodes in actual slag furnaces, one must be skeptical of the results predicted from simplistic physical, finite element or analytical modeling.

From the limited information available, it can be concluded that while a ratio of S_e in the range from $2.4\text{-}3.0D_e$ appears reasonable, it may well be that lower ratios (e.g. 2 or even less) can be used without significantly altering the furnace resistance, particularly in furnaces designed to operate with deep electrode immersions. This would potentially allow for a smaller furnace diameter, while maintaining some minimum electrode to wall gap determined by the true radius of the electrode's 'active' zone. The existing lack of knowledge of the true nature of heat development in slag furnaces, restricts our ability to correctly model the electrode 'active' zone and optimize the furnace design.

The minimum electrode to wall spacing is directly related to where and how heat is produced and where the heat performs work in the furnace. Based on the previous discussions on electrode spacing, the approximate size of the heat producing area (HPA) can be estimated, corresponding to an electrode 'active' zone of $2D_e$ and a total minimum diameter of $4.3D_e$:

$$\text{Approximate HPA} = \pi (S_e + 2D_e)^2/4 = \pi (4D_e/\sqrt{3} + 2D_e)^2/4 = 14.6D_e^2 \qquad (7)$$

Ideally all heat produced in the HPA should be used beneficially before it leaves the area. Equation (7) provides an estimate of the minimum possible furnace area required under theoretically ideal heat transfer conditions, i.e. minimal slag superheat leaving the HPA.

Furnace Diameter

Little information is available in the open literature regarding slag furnace dimensions, particularly for round furnaces. From the available literature, furnace diameters (D_f) ranging from $8D_e$ to $12D_e$ for round furnaces, appear to be typical [26-27]. Hence, one method of arriving at a furnace diameter is to multiply the selected electrode diameter by a value between 8 and 12. A large electrode diameter subsequently results in a large furnace diameter and the use of small diameter UHP graphite electrodes, would correspondingly result in a small furnace diameter and high power intensity (i.e. a 3rd or 4th generation furnace design).

Eric *et al.* have made one of the few systematic studies of slag furnace scaling parameters, as related to South African matte-precious group metal (PGM) smelting furnaces and how they may be related to electrical, thermal and viscous properties of the slag [6-7, 28]. Furnace diameters from 6 to $8.6D_e$ or a minimum electrode-to-wall spacing of 1.15 to $2D_e$ (measured from the electrode flank), were recommended based on estimates of slag superheat arriving at the side lining [7].

Using Eric's recommended electrode-wall spacing, the minimum (D_{fmin}) and maximum furnace diameter (D_{fmax}) can be estimated based on the previously discussed electrode spacings from 2-3D_e:

$$D_{fmin} = 2\ (2D_e)/\sqrt{3} + D_e + 2\ (1.15D_e) = 5.6D_e \quad (8)$$

$$D_{fmax} = 2\ (3D_e)\ /\sqrt{3} + D_e + 2\ (2D_e) = 8.5D_e \quad (9)$$

Optimum Furnace Diameter for Maximum Throughput

Alternatively, the furnace diameter can be defined by simply selecting a target energy intensity and total furnace power; however, this procedure is not likely to produce the 'optimum' design. The optimum slag furnace design is the one which will result in the highest throughput for any particular total furnace power input, i.e. the minimum kWh/mt of feed material.

Heat produced in the furnace does work in a number of ways:

1. Preheats charge,
2. Pre-reduces charge,
3. Melts charge,
4. Produces the superheat required to achieve tapping, and
5. Drives reduction reactions in the slag phase.

Any heat that is not consumed productively must necessarily leave the furnace as heat losses.

If the electrodes are placed too close to the copper coolers, then hot slag driven by buoyant forces will impinge directly on the coolers before it has an opportunity to transfer heat to the charge, and the furnace heat losses will be increased due to 'forced' convection. The optimum furnace diameter will correspond to the diameter of incipient impingement, i.e. the exact point of transition from natural to forced convection heat transfer at the wall. There is no accepted method to predict this required spacing. It may be that this can be determined using experimentally validated computational fluid dynamic models or by careful study of industrial furnaces.

As a first approximation when more heat is added to the furnace, for example to perform more melting, and assuming a fixed area of contact between the charge and slag and slag-charge heat transfer coefficient, the slag gets proportionately hotter as indicated in Equation (10):

$$Q_{slag\text{-}charge} = A_{slag\text{-}charge}\ h_{slag\text{-}charge}\ (T_{slag} - T_{liquidus}) = PR * SER \quad (10)$$

where: $Q_{charge\text{-}slag}$ is the amount of energy that must be transferred to heat (pre-reduce) and melt the charge [W], $A_{slag\text{-}charge}$ is the interfacial area between slag and charge [m^2], and $h_{slag\text{-}charge}$ is the overall slag-to-charge heat transfer coefficient (W/m^2/K), T_{slag} is the average temperature of the bulk slag under the charge [K], $T_{liquidus}$ is the liquidus temperature of the slag [K], *PR* [kg/h] and *SER* [Wh/kg] are the production rate and specific energy requirement as discussed previously.

From Equation (10) we see that the quantity of heat to be transferred from the slag-to-charge, will determine the required slag superheat. 100% Bath power, i.e. immersed electrodes are assumed. Arc power must be treated separately [29-30]. Energy consumed by reduction reactions will not significantly increase the superheat and can be excluded from the analysis. If the heat transfer coefficient in Equation (10) is large enough, then the slag temperature leaving the minimum area predicted by Equation (7) will approach some practical minimum temperature, corresponding to the 'ideal' slag superheat. In slag furnace operation, 50^{o}C of superheat is often considered the minimum to ensure good tapping based on the slag's viscosity. Slag superheats in excess of 200^{o}C are unusual in practice and are usually dictated by a process requirement (e.g. slag liquidus < metal liquidus).

At present, there is no reliable method to theoretically predict the heat transfer coefficient in Equation (10) and this is best accomplished as part of a pilot smelting campaign with feed as representative of the future industrial operation, or taken directly from an analogous industrial operation using similar or ideally identical feed material.

Typical heat losses at slag furnace sidewalls are in the range of 10-100 kW/m^2 and more commonly in the range of 10-50 kW/m^2 [29]. Heat losses depend on the furnace energy intensity, slag superheat, slag physical properties and furnace operating practice. In order to maintain a freeze lining, the sidewall cooler must remove all heat arriving at the hot face, and hence a heat flux boundary condition, rather than a temperature boundary condition (as in the case of an insulated wall) exists. The slag-wall heat flux [W/m^2] can then be calculated from the following equation [31]:

$$Q/A_{slag\text{-}wall} = h_{slag\text{-}wall}\,(T_{bulkslag} - T_{hotface}) \qquad (11)$$

where $Q_{slag\text{-}wall}$ is the heat loss [W], $A_{slag\text{-}wall}$ is the area of the coolers [m^2], $h_{slag\text{-}wall}$ is the slag to wall heat transfer coefficient [W/m^2/K], $T_{bulkslag}$ is the temperature of the bulk slag close to the wall [K] and $T_{hotface}$ is the temperature at the stagnant mushy zone of the hot-face [K].

Procedures for adequately predicting the side wall heat transfer coefficient have been published previously [31-32] based on the assumption that natural convection dominates the transfer of heat to the wall. The heat transfer coefficient in Equation (11) will be on the order of 250 W/m^2/K (e.g. 50000W/m^2/200K thermal driving force).

Sidewall heat losses estimated with Equation (11) will still increase with slag superheat as predicted by Equation (10). Under unusual operating conditions, a transition to forced convection may be experienced, e.g. due to bubble driven flow and the heat transfer coefficient may increase dramatically [33]. Heat fluxes used for cooler design must be based on peak emergency values and not nominal values. Nominal values should be used for heat balance calculations and predictions of annual capacity.

Examples

The principles discussed in this paper can be better understood by way of specific examples. Two 80 MW examples are shown in Table II. The first case is for a very large scale 2nd generation furnace operating with immersed electrodes (i.e. 100% bath power). The second case has been solved to find the furnace dimensions, which produce the maximum throughput for the same electrode diameter and total furnace power, as used in the first case.

'Pure' slag melting is assumed, i.e. no metal, reduction energy or off-gas. A slag heat capacity of 1.1 kJ/kg/K has been assumed [4]. It is assumed that there is 200°C difference between the liquidus and solidus of the slag and that the slag-wall heat transfer coefficient is 250 W/m^2/K. The furnace shell temperature has been assumed 200°C, the roof heat losses 4 kW/m^2, the upper sidewall losses 12 kW/m^2 and the hearth losses 10 kW/m^2 for the first case. Losses have been scaled in proportion to the thermal driving forces for the maximum throughput case (insulated condition). For the 2nd generation furnace an electrode spacing of 2.7D_e is assumed and for the maximum throughput case, the electrode spacing has been reduced to 2D_e. For the maximum throughput case the copper block heat fluxes and the furnace resistance have been scaled for the effect of the increased furnace energy intensity.

Table II. Examples of Furnace Dimensioning, 2nd Generation and Maximum Throughput

Furnace Parameters	2nd Generation Furnace	Maximum Furnace Throughput
Furnace Power, kW	80000	80000
Electrode Size, m	2	2
Electrode Number	3	3
Electrode Resistance, mohms	5.0	4.5
Electrode Current, kA	73.0	76.8
Electrode Current Density, A/cm^2	2.3	2.4
Furnace Power Intensity, kW/m^2	250	339
Furnace Area, m^2	320	236
Furnace Diameter, m	20.2	17.3
D_f/D_e	10.09	8.67
Electrode-Wall Spacing, (D_e)'s	2.99	2.68
Upper Wall Height, m	2	2
Slag Height, m	1	1
Slag-Wall Thermal Driving Force, ΔK	160	181
Copper Block Area, m^2	63.4	54.5
Copper Block Heat Flux, kW/m^2	40	45
Slag Super Heat, ΔK	60	81
Slag Liquidus, °C	1450	1450
Slag Solidus, °C	1250	1250
Slag Temperature, °C	1510	1531
Copper Block Heat Loss, kW	2537	2469
Other Heat Losses, kW	6002	4690
Total Heat Losses, kW	8538	7159
Heat Available For Smelting, kW	71462	72841
Thermal Efficiency, %	89.3	91.1
Throughput, mt/h	154.9	155.7

It can be observed that the maximum throughput case results in a 3rd generation furnace design, which has 1.8% higher thermal efficiency and 1% more throughput. Given the

smaller furnace foot print, one would assume such a furnace would be less expensive to construct. Scaling by area$^{0.6}$, would give an estimate of 17% less expensive. The copper block heat fluxes of 45 kW/m^2 are in the normal range. Electrode-wall spacing has not significantly changed, thereby reducing the risk of hot-slag impingement onto the wall.

Conclusions

Methods for systematically designing slag furnaces are restricted by our lack of fundamental understanding of the nature of heat production and heat transfer in slag furnaces. Simplistic models have been presented, which might be improved by targeted measurements in industrial slag furnaces. Further efforts should be undertaken to determine the real voltage gradients and complex impedances in industrial slag furnaces operating at low frequency (50-60 Hz) and high current with immersed electrodes. Greater effort should be expended to determine the radial temperature profile at the slag-charge interface, measured from the heat producing area out to the near wall region. Better furnace measurements might allow the creation of validated electrical and thermal models, improved analytical equations and optimized furnace designs.

References

1. M. Kennedy, H. Haaland, and J. A. Aune, "High Intensity Slag Resistance Furnace Design," presented at the Conference of Metallurgists, CIM, Sudbury, Ontario, (2009).
2. G. Ellefsen and Ø. Hallquist, "The Elkem Multi-Purpose Furnace® Used for Slag Production, Technical Description with Plant Features," presented at the Elkem seminar, Bhubaneswar, India, (1989).
3. G. Slaven, A. MacRae, and L. Valentas, "The Implementation of Ultralife™ Copper Casting Technology in the Eaf," Presented at AISE, Pittsburg, PA, (2003).
4. J. Matousek, "The Thermodynamic Properties of Slags," *JOM Journal of the Minerals, Metals and Materials Society,* vol. 60, (2008), 62-64.
5. M. W. Kennedy, M. Garcia, and F. Olesen, "Comparison of Classical Tools and Modern Finite Element Modeling in the Electrical Design of Slag Resistance Furnaces," submitted to the International Smelting Technology Symposium (Incorporating the 6th Advances in Sulfide Smelting Symposium), TMS, Orlando, Florida, (2012).
6. R. Eric and A. Hejja, "Dimensioning, Scale-up and Operating Considerations for Six Electrode Electric Furnaces. II. Design and Scale-up Considerations for Furnaces Treating Pgm-Containing Copper-Nickel Concentrates," EPD Congress, (1995), 239-257.
7. R. Eric, "Slag Properties and Design Issues Pertinent to Matte Smelting Electric Furnaces," *Journal of the South African Institute of Mining and Metallurgy,* vol. 104, (2004), 499-510.
8. C. W. Søderberg, Of Christiania, US Patent 1,440,724, (1923).
9. J. Westly, "Critical Parameters in Design and Operation of the Submerged Arc Furnace," *Electric Furnace Conference*, (1975), 47-53.
10. S. A. Halvorsen, A. M. Valderhaug, J. Fors, and E. A. S. A. Carbon, "Basic Properties of the Persson Type Composite Electrode," *Electric Furnace Conference*, (1999), 185-1204.
11. "Carbon Electrodes–Performance Products for Non-Ferrous Arc Furnace Applications," SGL Group, (2009).
12. R. S. Hogue, R. L. Westlake, and G. M. Moga, "Carbon and Graphite Electrodes Evaluated for Use in Ferroalloy Furnaces," *Journal of Metals,* (1954), 1379-1382.
13. L. Kelvin, *Mathematical Papers, Vol. 3*, (London: Cambridge University Press, 1890), 484-515.
14. N. McLachlan, *Bessel Functions for Engineers*, (Gloucestershire: Clarendon Press, 1955).

15. H. Larsen, "Current Distribution in the Electrodes of Industrial Three-Phase Electric Smelting Furnaces," Proceedings of the 2006 Nordic COMSOL Conference, Copenhagen, Denmark, 20 November, (2006).
16. "Maximizing Steel Productivity through Technology and Service Leadership," Graftech, (2005), 1-19.
17. "Graphite Electrodes - Ultrahigh-Performance Electrodes - A New Dimension in Productivity," SGL Carbon Group, (2005), 1-19.
18. Z. B. Wowk, "Characteristics of a Submerged-Arc Furnace," *Electric Furnace Conference*, (1964), 158-160.
19. A. Shkirmontov, "Comparison of the Parameters of Ferrosilicon-Smelting Furnaces with Different Electrode Spacings," *Metallurgist,* (2011), 1-5.
20. A. Shkirmontov, "Energy Parameters of Ferrosilicon Production with Larger-Than-Normal Values for the Electrode Gap and Electrode Spacing under Factory Conditions," *Metallurgist,* vol. 53, (2009), 642-647.
21. A. Shkirmontov, "Determination of the Energy Parameters for the Smelting of Manganese Ferroalloys with Increases in the Electrode Gap and Electrode Spacing," *Metallurgist,* vol. 53, (2009), 512-517.
22. R. Urquhart, M. Rennie, and C. Rabey, "The Smelting of Copper-Nickel Concentrates in an Electric Furnace," *Extractive Metallurgy of Copper*, (1976), 274-295.
23. Q. Jiao, "Generation and Transmission of Heat in an Electric Slag Resistance Furnace," Ph.D. Thesis, Columbia University, New York, New York, USA, (1991), 222.
24. Y. Sheng, G. Irons, and D. Tisdale, "Transport Phenomena in Electric Smelting of Nickel Matte: Part I. Electric Potential Distribution," *Metallurgical and Materials Transactions B,* vol. 29, (1998), 77-83.
25. M. Manvelyan, A. Melik-Ankhazaryan, K. Kostanyan, and S. Nalchadzhyan, "The Use of Graphite Electrodes in Electrically Heated Glass Furnaces," *Glass and Ceramics,* vol. 13, (1956), 297-303.
26. K. Donadson, F. Ham, and R. Francki, "Design of Refractories and Bindings for Modern High-Productivity Pyrometallurgical Furnaces," Canadian Institute of Mining, Metallurgy and Petroleum, vol. 36, #971, (1992), 112-118.
27. S. King, "Electric Smelting Furnaces in Southern Africa," *Proceedings of INFACON 74,* South African Institute of Mining and Metallurgy, Johannesburg, (1975), 135-142.
28. R. H. Eric, "The Importance of the Slag Phase in Electric Smelting of PGM Containing Sulphide Concentrates," presented at the Sohn International Symposium, (2006), 559-582.
29. C. Walker, T. Koehler, N. Voermann, and B. Wasmund, "High Power, Shielded-Arc FeNi Furnace Operation - Challanges and Solutions," The Twelfth International Ferroalloys Congress, Helsinki, Finland, 6-9 June, (2010), 681-696.
30. N. Voermann, T. Gerritsen, I. Candy, F. Stober, and A. Matyas, "Furnace Technology for Ferro-Nickel Production - an Update," International Laterite Nickel Symposium, Charlotte, NC, USA, 14-18 March, (2004), 563-577.
31. H. Joubert, "Designing for Slag "Freeze Linings" on Furnace Sidewalls – an Engineering Perspective," Molten Slags, Fluxes and Salts, Stockholm, Eds. S. Seetharaman and D.U. Sichen, Sweden-Helsinki, 12-17 June, (2000).
32. S. Kang, "A Model Study of Heat Transfer and Fluid Flow in Slag-Cleaning Furnaces," Ph.D. Thesis, University of Missouri-Rolla, Rolla, Missouri, USA, (1991), 182.
33. L. Nelson, R. Sullivan, P. Jacobs, E. Munnik, P. Lewarne, E. Roos, M. Uys, B. Salt, M. de Vries, and K. McKenna, "Application of a High Intensity Cooling System to DC-Arc Furnace Production of Ferrocobalt at Chambishi," *SAIMM Journal,* vol. 104, (2004), 551-561.